

# Modeling the frequency dependence (5–120 MHz) of ultrasound backscattering by red cell aggregates in shear flow at a normal hematocrit

Isabelle Fontaine<sup>a)</sup> and Guy Cloutier<sup>b)</sup>

Laboratory of Biorheology and Medical Ultrasonics, Research Center, University of Montreal Hospital, Notre-Dame Hospital, 2099 Alexandre de Sève (room Y-1619), Montréal, Québec H2L 2W5, Canada and Department of Radiology, Radio-Oncology and Nuclear Medicine, University of Montreal, C.P. 6128, Succ. Centre-ville, Montréal, Québec H3C 3J7, Canada

(Received 18 November 2002; accepted for publication 3 February 2003)

The frequency dependence of the ultrasound signal backscattered by blood in shear flow was studied using a simulation model. The ultrasound backscattered signal was computed with a linear model that considers the characteristics of the ultrasound system and tissue acoustic properties. The tissue scattering properties were related to the position and shape of the red blood cells (RBCs). A 2D microrheological model simulated the RBC dynamics in a Couette shear flow system. This iterative model, described earlier [Biophys. J. **82**, 1696–1710 (2002)], integrates the hydrodynamic effect of the flow, as well as adhesive and repulsive forces between RBCs. RBC aggregation was simulated at 40% hematocrit and shear rates of  $0.05$ – $2 \text{ s}^{-1}$ . The RBC aggregate sizes ranged, on average, from 3.3 RBCs at  $2 \text{ s}^{-1}$  to 33.5 cells at  $0.05 \text{ s}^{-1}$ . The ultrasound backscattered power was studied at frequencies between 5–120 MHz and insonification angles between  $0$ – $180^\circ$ . At frequencies below approximately 30 MHz, the ultrasound backscattered power increased as the shear rate was decreased and the size of the aggregates was raised. A totally different scattering behavior was noted above 30 MHz. Typical spectral slopes of the backscattered power (log–log scale) between 5–25 MHz equaled 3.8, whereas slopes down to 0.6 were measured at  $0.05 \text{ s}^{-1}$ , between 40–60 MHz. The ultrasound backscattered power was shown to be angle dependent at low frequencies (5–25 MHz). The anisotropy persisted at high frequencies ( $>25 \text{ MHz}$ ) for small aggregates (at  $2 \text{ s}^{-1}$ ). In conclusion, this study sheds some light on the blood backscattering behavior with an emphasis on the non-Rayleigh regime. Additional experimental studies may be necessary to validate the simulation results, and to fully understand the relation between the ultrasound backscattered power, level of RBC aggregation, shear rate, frequency, and insonification angle. © 2003 Acoustical Society of America. [DOI: 10.1121/1.1564606]

PACS numbers: 43.80.Cs, 43.80.Jz, 43.80.Qf [FD]

## I. INTRODUCTION

The backscattering of an acoustic wave by a linear biological tissue is governed by the size of the tissue microstructure with respect to the acoustic wavelength, and by the acoustical impedance mismatches produced by the tissue inhomogeneities. Weakly scattering particles much smaller than the wavelength are referred to as Rayleigh scatterers. The power backscattered by randomly distributed Rayleigh scatterers is known to increase with the fourth power of the incident wave frequency. In contrast, scattering by reflectors of dimension much larger than the wavelength is generally frequency independent. Intermediate sizes of biological scatterers from various tissues were shown to be characterized by a wide range of frequency dependence ( $f^0$  to  $f^{4.5}$ , approximately).<sup>1–3</sup> Even greater dependencies (up to  $f^6$ ) were predicted for densely packed scatterers.<sup>4</sup> For small particles with respect to the wavelength, the deviation from the Rayleigh scattering theory ( $f^4$ ) can be explained by the existence of organized patterns diminishing the randomness in the positioning of the biological scattering cells.

Within the last 25 years, several studies have aimed at elucidating the backscattering of ultrasound by blood. Rayleigh scattering was observed, between 3.5 and 12.5 MHz, for suspensions of nonaggregating red blood cells (RBCs) washed and resuspended in a saline solution to eliminate the plasma proteins responsible for the aggregation.<sup>5</sup> The spectral slope of the backscattering coefficient for a suspension of nonaggregating bovine RBCs was 3.95, when corrected for attenuation (a slope of 4.0 was theoretically expected). In contrast, the frequency dependence of porcine whole blood at a low shear rate was lower in the same range of frequencies, presumably because of the presence of RBC aggregates<sup>5</sup> (shear rates below  $\approx 1 \text{ s}^{-1}$  promote the aggregation of RBCs, and RBC aggregates may still exist up to  $\approx 50 \text{ s}^{-1}$  and even higher shear rates under pathological conditions<sup>6</sup>).

At higher frequencies (22–37 MHz), a mean spectral slope around 1.0 (not corrected for the frequency-dependent attenuation) was measured for normal human whole blood flowing at a low shear rate.<sup>7</sup> At these frequencies, the spectral slope for suspensions of nonaggregating RBCs differed from the Rayleigh scattering theory (slope  $\approx 3.0$ ). Similar spectral slopes (1.3–1.4, attenuation compensated) to those found by Van der Heiden *et al.*<sup>7</sup> were reported, between

<sup>a)</sup>Ms. Fontaine left the laboratory in 2001. She is now with ORTHOsoft, Inc., Montréal, Canada.

<sup>b)</sup>Electronic mail: guy.cloutier@umontreal.ca

35–65 MHz, for normal human blood circulating in a flow phantom.<sup>8</sup> Foster *et al.*<sup>9</sup> measured an attenuation compensated spectral slope as low as 0.4, between 40–60 MHz, for normal human blood sheared in a Couette flow at  $0.16 \text{ s}^{-1}$ . In the above studies,<sup>5,7–9</sup> the hematocrit was in the normal physiological range (between 35%–45%). Hematocrit changes well beyond normal physiological values can affect the spectral slope of the backscattering coefficient.<sup>5</sup> Other factors such as the temperature, flow shearing condition, and plasma protein contents must be known if one attempts to systematically compare the spectral slope of the backscattering coefficient from blood.

Particles of the size of an RBC can be considered Rayleigh scatterers when insonified by a plane wave at frequencies below 30 MHz, approximately.<sup>10</sup> However, backscattering by blood cannot simply be described by considering independently distributed finite scatterers. Blood is characterized by a high number density of RBCs that are subjected to various levels of aggregation under flowing condition. As a consequence, this implies various structural arrangements of RBCs, and thus various patterns of acoustic interference between the different scattered echoes. According to recent models,<sup>10–12</sup> the frequency dependence of the backscattered signal from blood depends not only on the scatterers' size, but also on their spatial arrangement. Savéry and Cloutier<sup>12</sup> developed an analytical backscattering model based on the Neyman–Scott random point process, predicting the frequency dependence of aggregating particles at a low hematocrit (<5%). The purpose of the present study is to extend these results to a normal physiological hematocrit by considering the shearing effect of the flow on the RBC spatial organization.

## II. METHODS

As performed earlier,<sup>13</sup> RBC aggregates can be viewed as large distinct scatterers containing numerous cells. However, a more effective way to model the backscattering properties is to consider individual RBCs, identical in shape, whose positions vary in space with the hematocrit and the level of aggregation. This approach was recently adopted to study the effect of the shear rate and anisotropy on ultrasound backscattering by aggregating RBCs at 10 MHz.<sup>14</sup> The backscattered signal was predicted by considering the ultrasonic transducer properties, the backscattering cross section of a single cell, and the spatial arrangement of RBCs.

The simulation model used in the present study is described in detail elsewhere.<sup>14</sup> In summary, the radio-frequency (rf) signal backscattered by blood was modeled in two dimensions by the following equation:

$$\text{rf}(x,y) = \frac{\partial^2}{\partial y^2} T(x,y) \otimes C(x,y) \otimes N(x,y), \quad (1)$$

where  $y$  is the direction of propagation of the ultrasonic waves perpendicular to the flow direction  $x$ ,  $T(x,y)$  is the ultrasound system transfer function,  $C(x,y)$  represents the spatial inhomogeneity due to a single RBC, and  $N(x,y)$  is the microscopic density function describing the RBC positioning. The transducer transfer function ( $T$ ) was modeled as

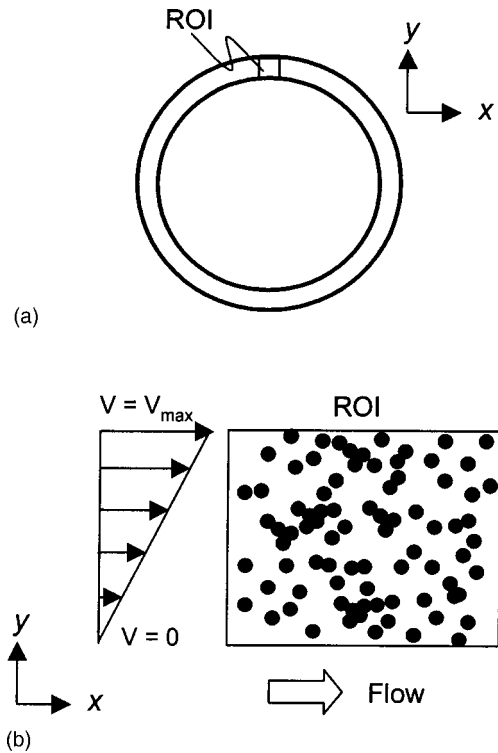


FIG. 1. (a) Top view of the two coaxial cylinders composing the Couette flow system. The region of interest (ROI) is located in the small gap between the two cylinders. The  $x$  axis refers to the direction of the flow parallel to the cylinders, and the  $y$  axis refers to the radial direction between the cylinders. (b) Magnification of the ROI and illustration of the velocity profile, assuming a constant shear rate in the ROI.

a Gaussian envelope modulated by a cosine function

$$T(x,y) = \exp\left[-\frac{1}{2}\left(\frac{x^2}{\psi_x^2} + \frac{y^2}{\psi_y^2}\right)\right] \cos\left(\frac{4\pi fy}{c}\right), \quad (2)$$

where  $\psi_x$  and  $\psi_y$  are the standard deviations of the 2D Gaussian function representing the beamwidth and the bandwidth of the transmitted waves. They were kept constant to  $\psi_x = 0.43 \text{ mm}$  and  $\psi_y = 0.03 \text{ mm}$  for all frequencies studied. The selected value of  $\psi_y$  corresponds to a bandwidth of approximately 10 MHz at  $-3 \text{ dB}$ . The parameter  $f$  in Eq. (2) is the ultrasonic frequency and  $c$  is the speed of sound in blood (1570 m/s).

The function  $C$  in Eq. (1) was defined as the 2D projection of a  $5.5\text{-}\mu\text{m}$ -diameter sphere [Eq. (11) of Fontaine *et al.*<sup>14</sup>]. The function  $N$  was obtained from 2D dynamical simulations of the RBC aggregation process in a shear flow.<sup>14</sup> It consists of an iterative microrheological model that considers the effect of the adhesive and repulsive forces between RBCs, and the hydrodynamic effect of the flow shear rate on the positioning of the particles. The motion of the particles resulting from the flow was between two coaxial cylinders (Couette flow—see Fig. 1), where the shear rate is maintained constant for a given relative rotational speed of one of the two cylinders. Shear rates varying between  $0.05$  and  $2 \text{ s}^{-1}$  were modeled. Different levels of aggregation were obtained by modifying the balance of forces acting on RBCs under physiological conditions (adhesion due to adsorption or depletion of plasma macromolecules between neighboring RBCs, repulsion due to steric and electrostatic

TABLE I. Effect of the shear rate on the mean numbers of RBCs per aggregate, and on the slopes of the frequency dependence of the ultrasound backscattered power between 5–25 MHz and 40–60 MHz (means  $\pm$  s.d.,  $n=8$ ). The spectral slopes were obtained for an insonification angle of  $90^\circ$  with respect to the flow.

Shear rate ( $s^{-1}$ )	Number of RBCs per aggregate	Spectral slope (5–25 MHz)	Spectral slope (40–60 MHz)
0.05	$33.5 \pm 2.4$	$3.3 \pm 0.3$	$0.6 \pm 1.1$
0.1	$23.0 \pm 2.2$	$3.3 \pm 0.2$	$0.9 \pm 1.0$
0.3	$11.9 \pm 0.2$	$3.4 \pm 0.1$	$3.4 \pm 1.0$
2	$3.3 \pm 0.1$	$3.1 \pm 0.2$	$3.6 \pm 0.7$

<sup>a</sup> $p < 0.001$ .

forces, and the effect of the flow). In the present study, the simulated conditions are limited to the intermediate level of aggregation described by Fontaine *et al.*<sup>14</sup> All simulations were performed in an area of 300 by 300  $\mu\text{m}$  at a hematocrit of 40%, which gives approximately 1500 particles in the region of interest (ROI). At each time step considered, the vector displacements resulting from each force (adhesion, repulsion, and flow) were summed for every RBC included between the two coaxial cylinders. Once the displacements were computed for all particles, they were moved for the next iteration. Starting with randomly positioned nonaggregated particles at the first iteration, the process was continued until the size of the aggregates reached a steady state (stable aggregate size—see Fig. 5 of Fontaine *et al.*<sup>14</sup>).

The backscattered power was computed from the 2D spectrum of the rf images obtained by Eq. (1). The spectrum of the rf image was evaluated from the central portion (256 by 256  $\mu\text{m}$ ) of the simulated ROI to avoid errors from the edges (the boundaries could promote the formation of artificial aggregate structures). The backscattered power (POW) was determined for the steady state of aggregation by

$$\text{POW} = \frac{1}{M_S} \sum_{f_x} \sum_{f_y} \left| \mathfrak{F} \left( \frac{\partial^2}{\partial y^2} T \right) \mathfrak{F}(C) \mathfrak{F}(N) \right|^2, \quad (3)$$

where  $M_S$  is the number of samples in the frequency domain ( $f_x, f_y$ ). For a given simulation, the spectra of five functions  $N$  (i.e.  $\mathfrak{F}(N)$ ), taken at the steady state of aggregation, were averaged to reduce the statistical variance. Then, the backscattered power obtained from Eq. (3) was computed and averaged over eight simulations performed under the same conditions. The initial random positioning of nonaggregated and nonoverlapped RBCs was changed between simulations, thus resulting in different aggregate structures.

TABLE II. Effect of the insonification angle, for a shear rate of  $0.05 s^{-1}$ , on the slopes of the frequency dependence of the ultrasound backscattered power between 5–25 MHz and 40–60 MHz (means  $\pm$  s.d.,  $n=8$ ).

Angle (degrees)	Spectral slope (5–25 MHz)	Spectral slope (40–60 MHz)
0	$2.6 \pm 0.2$	$1.2 \pm 0.4$
45	$2.7 \pm 0.4$	$1.6 \pm 0.7$
90	$3.3 \pm 0.3$	$0.6 \pm 1.1$
135	$2.7 \pm 0.2$	$1.3 \pm 0.4$

<sup>a</sup> $p < 0.001$ .

<sup>b</sup> $p = 0.002$ .

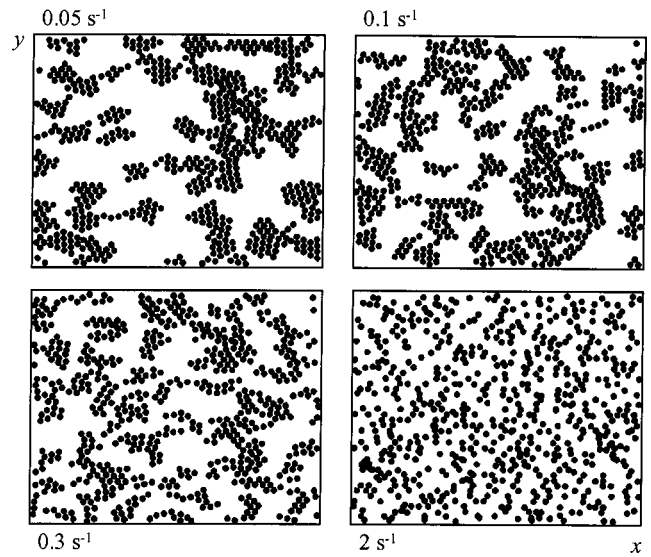


FIG. 2. Simulation results of RBC aggregation at 40% hematocrit for shear rates of 0.05, 0.1, 0.3, and  $2 s^{-1}$ . The simulated areas are 300 by 300  $\mu\text{m}$ , and the zoomed areas represent a dimension of 200 by 200  $\mu\text{m}$ . Each panel was obtained at the steady state of aggregation of the iterative microrheological model. The  $x$  and  $y$  coordinates correspond to the direction of the flow and of the radial direction between the cylinders of the Couette flow system, respectively.

To allow the study of the anisotropy of the backscattered power, the rf signal was modeled at various angles of insonification by doing a rotation of the transducer transfer function. As performed earlier,<sup>13,14</sup> the  $x$ – $y$  plane was mapped onto the  $p$ – $q$  plane. The function characterizing the transducer was computed on the rotated axes. The following equations were used to transform the  $x$ – $y$  plane onto the  $p$ – $q$  plane:

$$\begin{bmatrix} p \\ q \end{bmatrix} = \begin{pmatrix} \sin \theta & \cos \theta \\ -\cos \theta & \sin \theta \end{pmatrix} \begin{bmatrix} x \\ y \end{bmatrix}, \quad (4)$$

where  $\theta$  represents the angle of rotation of the axes. Thus,  $0^\circ$  and  $90^\circ$  correspond, respectively, to a direction of insonification parallel and perpendicular to the flow  $x$ .

### A. Statistical analyses

All results were expressed as means  $\pm$  standard deviations (s.d.). One-way analyses of variance with Bonferroni's method for multiple comparisons were used to assess the differences in the mean aggregate sizes and spectral slopes listed in Tables I and II (SIGMASTAT statistical software, version 2.0, SPSS Science, Chicago, IL). A significance level of 0.05 was considered in all analyses.

## III. RESULTS

A key feature of the current model is the possibility to simulate various RBC aggregate structures and the corresponding ultrasound backscattered signal in response to the shear rate intensity. Figure 2 shows examples of RBC spatial arrangements obtained at the steady state of aggregation (after more than 15 000 iterations), for shear rates of 0.05, 0.1, 0.3, and  $2 s^{-1}$  and a hematocrit of 40%. As expected, the fraction of aggregated RBCs and the size of the aggregates increased as the shear rate was decreased. At low shear rates

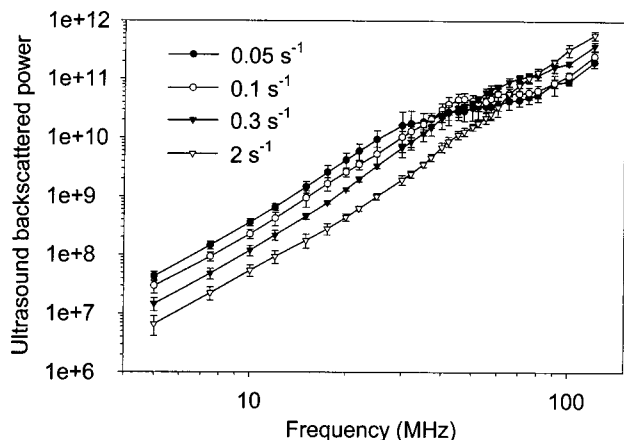


FIG. 3. Frequency dependence of the ultrasound backscattered power (relative units, means  $\pm$  s.d.,  $n=8$ ) at an insonification angle of  $90^\circ$  with respect to the flow, for shear rates of 0.05, 0.1, 0.3, and  $2 \text{ s}^{-1}$ .

(e.g.,  $0.05$  and  $0.1 \text{ s}^{-1}$ ), clump types of aggregates were obtained with the model. The compactness of the aggregates increased as the shear rate was decreased. Rouleaux of a few RBCs were more often observed at higher shear rates (e.g.,  $2 \text{ s}^{-1}$ ).

The frequency dependencies of the ultrasound backscattered power at an insonification angle of  $90^\circ$  with respect to the flow are presented in Fig. 3, for shear rates of 0.05, 0.1, 0.3, and  $2 \text{ s}^{-1}$ . At frequencies below approximately 30 MHz, the ultrasound backscattered power increased as the shear rate was decreased and the level of aggregation was raised. The mean increase of the backscattered power between shear rates of 0.05 and  $2 \text{ s}^{-1}$  was  $9.1 \pm 1.2 \text{ dB}$ . The mean numbers of RBCs per aggregate at these shear rates were 33.5 ( $0.05 \text{ s}^{-1}$ ), 23.0 ( $0.1 \text{ s}^{-1}$ ), 11.9 ( $0.3 \text{ s}^{-1}$ ), and 3.3 ( $2 \text{ s}^{-1}$ ) (see Table I,  $p < 0.001$ ). As also seen in Table I, the slopes on a log-log scale of the frequency dependence of the backscattered power, between 5–25 MHz, were independent of the shear rate (mean values around 3.3,  $p = 0.06$ ).

Above 30 MHz, a totally different scattering behavior was observed in Fig. 3. The backscattered power was no longer positively correlated with the mean size of the aggregates, or inversely with the shear rate. For instance, at a given shear rate, changes in the slope of the backscattered power as a function of frequency were noted. As emphasized in Table I, the slope at  $0.05 \text{ s}^{-1}$  was 3.3 between 5–25 MHz, and decreased to 0.6 between 40–60 MHz. At higher shear rates between 40–60 MHz, the slope increased from 0.9 at  $0.1 \text{ s}^{-1}$  to 3.6 at  $2 \text{ s}^{-1}$  ( $p < 0.001$ ). Because the change in the slope was more pronounced at  $0.05 \text{ s}^{-1}$  than at other shear rates, the backscattered power was lower at  $0.05 \text{ s}^{-1}$  than at  $0.1 \text{ s}^{-1}$  above 37 MHz, was lower at  $0.05 \text{ s}^{-1}$  than at  $0.3 \text{ s}^{-1}$  above 45 MHz, and was lower at  $0.05 \text{ s}^{-1}$  than at  $2 \text{ s}^{-1}$  above 65 MHz (see Fig. 3). The frequency at which the transition in the slope occurred increased as a function of the shear rate.

According to the Rayleigh scattering theory for particles much smaller than the acoustic wavelength (particle, continuum, or hybrid modeling approaches), the backscattering properties are independent of the insonification angle.<sup>15</sup> To verify the validity of the current model, in terms of angular

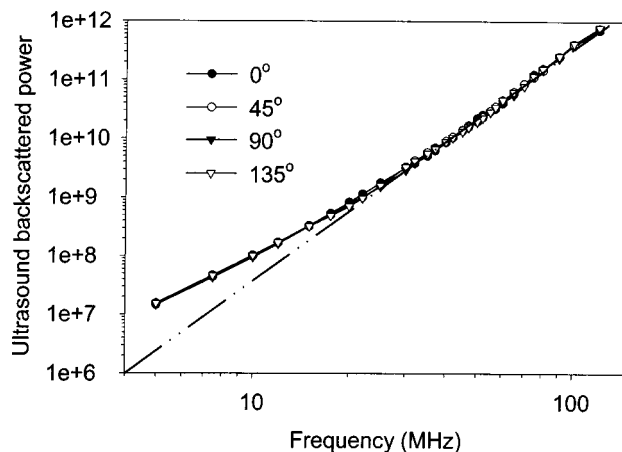


FIG. 4. Frequency dependence of the ultrasound backscattered power (relative units) for the initial random positioning of nonaggregated and nonoverlapped RBCs, at different insonification angles with respect to the flow. The dash-dotted line represents the theoretical fourth-power frequency relationship of Rayleigh scattering.

independencies for a scatterer's diameter of  $5.5 \mu\text{m}$  and a cell concentration of 40%, the backscattered power was estimated from the initial random positioning of nonaggregated and nonoverlapped RBCs (before the first iteration of the microrheological dynamical model of RBC aggregation). The spectra of the function  $N$  in Eq. (3) were averaged over 50 independent RBC realizations performed over the simulated area of 300 by 300  $\mu\text{m}$ , and the backscattered power was then computed for each frequency considered. As shown in Fig. 4, the insonification angle had no effect on the ultrasound backscattered power. However, the spectral slope of the backscattered signal differed, in the lower frequency range, from the fourth-power frequency dependence predicted by the Rayleigh scattering theory. The reasons for this discrepancy are postulated in Sec. IV.

The possible influence of the insonification angle on the ultrasound signal backscattered by aggregating RBCs was also investigated over the range of frequencies considered (see Fig. 5, shear rate =  $0.05 \text{ s}^{-1}$ ). It can be recalled that an angle of  $0^\circ$  refers to a direction of propagation of the ultrasound beam parallel to the flow, whereas  $90^\circ$  corresponds to

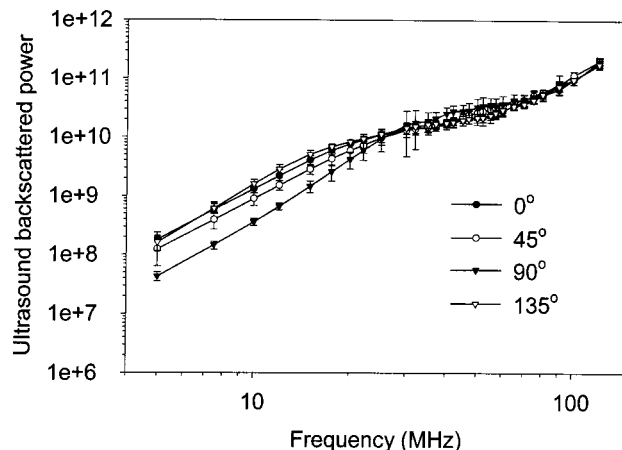


FIG. 5. Frequency dependence of the ultrasound backscattered power (relative units, means  $\pm$  s.d.,  $n=8$ ) for a shear rate of  $0.05 \text{ s}^{-1}$ , at different insonification angles with respect to the flow.

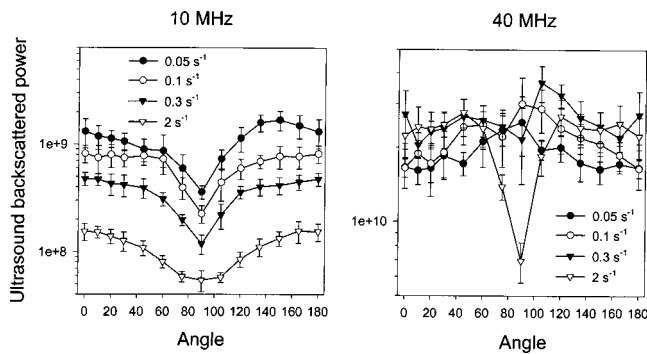


FIG. 6. Changes in the ultrasound backscattered power (relative units, means  $\pm$  s.d.,  $n=8$ ) as a function of the insonification angle, for shear rates of 0.05, 0.1, 0.3, and  $2 \text{ s}^{-1}$ , and mean frequencies of 10 and 40 MHz.

a perpendicular orientation. Significant variations of the backscattered power as a function of the insonification angle were noted at frequencies between 5–20 MHz, approximately. At  $90^\circ$ , the backscattered power was consistently lower than the values observed at the other angles. The strongest backscattering was noted at  $0^\circ$  and  $135^\circ$ . The maximum difference in the mean backscattered power as a function of the insonification angle was 6.5 dB (at 10 MHz). Between 25–120 MHz, the ultrasound backscattered power was angle independent for that low shear rate of  $0.05 \text{ s}^{-1}$ . Table II shows the effect of the insonification angle on the spectral slopes at the same shear rate value of  $0.05 \text{ s}^{-1}$ . Statistically significant differences ( $p < 0.005$ ) were observed between 5–25 MHz. At higher frequencies (40–60 MHz), the spectral slopes were similar on average ( $p = 0.06$ ).

Figure 6 is presented to further emphasize the relationship between the ultrasound backscattered power, insonification angle, shear rate (aggregation level), and frequency. At 10 MHz, the anisotropy (angular dependence) of the ultrasound backscattered power was relatively similar as a function of the shear rate. The range of variation of the mean backscattered power as a function of the angle was 6.7 dB at  $0.05 \text{ s}^{-1}$ , 5.6 dB at  $0.1 \text{ s}^{-1}$ , 6.0 dB at  $0.3 \text{ s}^{-1}$ , and 4.6 dB at  $2 \text{ s}^{-1}$ . For each shear rate, the minimum backscattering was found at an angle of  $90^\circ$ . With the exception of the shear rate at  $2 \text{ s}^{-1}$ , the anisotropic behavior of the backscattered power was more erratic at 40 MHz. As for the observation made at 10 MHz, the anisotropic behavior at  $2 \text{ s}^{-1}$  was characterized by a minimum of the backscattered power at  $90^\circ$ , and a range of variation of 6.0 dB. For the other shear rates and a frequency of 40 MHz, the angular variations were below 2.6 dB.

#### IV. DISCUSSION

A common belief, based on experimental observations and the Rayleigh scattering theory, is to consider that an increase in the level of RBC aggregation results in a raise of the ultrasound backscattered signal strength.<sup>16</sup> The simulation results presented in Fig. 3, at frequencies below 30 MHz, are consistent with this postulation because the backscattered power is shown to increase with a reduction of the shear rate and an increase in the size of the aggregates (see Table I). According to the Rayleigh scattering theory, a linear

increase in the backscattering coefficient (a measure proportional to the backscattered power) as a function of the scatterers' volume is expected, for a constant hematocrit and a spatial organization not affected by the scatterers' size.<sup>1,10</sup> According to Table I and Fig. 3, the simulation results seemed to deviate slightly from this prediction. As listed in Table I, the mean volume of RBC aggregates increased by a factor of 10.2 between shear rates of 2 and  $0.05 \text{ s}^{-1}$ . For the same shear rate changes, the backscattered power at  $90^\circ$  increased, on average, by a factor of only 8.1 (9.1 dB) below 30 MHz. Although this difference may be attributed to the variance of the simulated results, the fact that RBC aggregation influences the structure factor, a main determinant of the ultrasound backscattering properties, may also be a reasonable explanation. It can be recalled that the structure factor reflects the spatial organization (pair correlation) of scatterers in the frequency domain.<sup>12,14,17</sup> The spatial arrangement of RBCs due to aggregation had an influence on the backscattered power at frequencies below 30 MHz, but as seen in Fig. 3, the impact of the structure factor was more dominant at frequencies between 30–120 MHz (non-Rayleigh regime), as reflected by the changes in spectral slopes.

#### A. Effect of the insonification angle

Another common belief is to consider the backscattering from blood (with or without RBC aggregates) possibly angle dependent only in the non-Rayleigh regime.<sup>18,19</sup> It may be worth mentioning that although judged negligible by the authors, Kuo and Shung<sup>19</sup> predicted slight differences in magnitude of the backscattering cross section (backscattering from a single particle) between sphere, disk, and biconcave disk having the size of a RBC below 30 MHz, by using the T-matrix method. In the current study, the anisotropy of the backscattered power at frequencies below 25 MHz (expected Rayleigh regime) and a shear rate of  $0.05 \text{ s}^{-1}$  was not negligible and reached values up to 6.5 dB (see Fig. 5). As shown in Fig. 6, the shear rate did not seem to affect the anisotropy at low frequencies. Surprisingly, at a first glance, the anisotropy disappeared in the non-Rayleigh regime (frequencies above 25 MHz) for shear rates promoting the formation of large RBC aggregates. This may be explained by the structure of RBC aggregates simulated in Couette flow, which had more the form of clusters than oriented rouleaux at low shear rates (see Fig. 2). Another observation that can be made from Figs. 5 and 6 is the maximum backscattering, at low frequencies, that generally occurred at angles close to  $0^\circ$  or  $180^\circ$ . This would suggest that the privileged macroscopic orientation of the blood structure was close to parallel with the ultrasound beam in these simulations. In summary, to fully understand the relationship between the ultrasound backscattered power, insonification angle, and frequency, one needs to refer to the frequency dependence of the structure factor, as performed by Fontaine *et al.*<sup>14</sup> Additional experimental validations would be necessary to better understand the anisotropic behavior of the backscattered power from blood as a function of the frequency. To our knowledge, the only experimental results available were performed at 10 MHz.<sup>18</sup>

## B. Deviation from the fourth-power frequency dependence under Rayleigh scattering

As observed in Fig. 4, the frequency dependence of the backscattered power from nonaggregated and nonoverlapped RBCs, at a hematocrit of 40%, differed from the fourth-power relationship in the lower frequency range. This is clearly an artifact of the simulation model related to the filtering induced by the frequency response of the point spread function [Eq. (2)]. In theory, the incident wave should be plane and monochromatic (Dirac impulse in the frequency domain) to validate the definition of the backscattering coefficient.<sup>1</sup> In the current study,  $\psi_y$  in Eq. (2) was kept constant to 0.03 mm whatever the frequency studied. This resulted in a bandwidth of the point spread function, at  $-3$  dB, of 10 MHz (or relative bandwidths varying between 200% to 8.3% between 5–120 MHz). There were three main reasons to select a bandwidth of 10 MHz. It first allowed the transmitted power to remain constant whatever the frequency selected. Second, the constant value of  $\psi_y=0.03$  mm allowed us to constrain the size of the point spread function entirely within the ROI. But, more importantly, this bandwidth was selected to reduce the variance of the backscattered power computation as a function of the frequency. For instance, averaging was performed by computing, with Eq. (3), the backscattered power over  $f_y$  frequency samples. A smaller bandwidth would have required several additional realizations of the function  $N$  (the positioning of RBCs, as illustrated in Fig. 2) to obtain acceptable standard deviations. The obtaining of the functions  $N$  used to compute the backscattered power with Eq. (3) could necessitate several days (on a Pentium III computer) because up to 30 000 iterations could be required to obtain the steady state of aggregation with the microrheological model.

To estimate the bias induced in the low-frequency range (5–25 MHz) with the current model, additional simulations were performed by using a single RBC in the middle of the ROI. For such simulations, a fourth-power frequency dependence should be obtained. We did not evaluate the bias of the spectral slopes from the results of Fig. 4 because the random positioning of a large number of nonoverlapped and nonaggregated scatters is constrained by the exclusion volume effect (in theory, the spectral slope for such cases could be higher than 4.0<sup>20,21</sup>). By performing the simulations over individual RBCs with the current definition of the point spread function, the mean spectral slope had a value of 3.5 instead of 4.0 between 5–25 MHz (the slope was 4.0 between 40–60 MHz). Table III presents the corrected values of the spectral slopes as a function of the shear rate. To do so, a value of 0.5 was added to the results of Table I between 5–25 MHz. As seen in Table III, values closer to 4.0 were obtained in the low-frequency range. Thus, for the simulated conditions of RBC aggregation, close to Rayleigh scattering was obtained between 5–25 MHz, whatever the shear rate ( $p=0.06$ ). The corrections performed in Table III can also be applied to modify the results of Table II (new table not shown). In the low-frequency range, the corrected mean values of the spectral slopes would thus vary between 3.1 and 3.8 as a function of the insonification angle.

TABLE III. Spectral slopes between 5–25 MHz and 40–60 MHz (means  $\pm$  s.d.,  $n=8$ ), corrected for the bias induced by the broadband frequency response of the transducer, as a function of the shear rate (a value of 0.5 was added to the results of Table I between 5–25 MHz). The spectral slopes were obtained for an insonification angle of  $90^\circ$  with respect to the flow. Note that the same corrections could be performed with Table II (results not shown).

Shear rate ( $s^{-1}$ )	Spectral slope (5–25 MHz)	Spectral slope (40–60 MHz)
0.05	$3.8 \pm 0.3$	$0.6 \pm 1.1$
0.1	$3.8 \pm 0.2$	$0.9 \pm 1.0$
0.3	$3.9 \pm 0.1$	$3.4 \pm 1.0$
2	$3.6 \pm 0.2$	$3.6 \pm 0.7$

## C. Effect of RBC aggregation on the spectral slopes

Experimentally, Rayleigh scattering was observed for nonaggregating RBCs at frequencies below 30 MHz (hematocrits = 6%–44%, attenuation-compensated backscattering coefficient).<sup>5,19</sup> In the presence of RBC aggregation for frequencies slightly above 10 MHz, spectral slopes below 4.0 were found.<sup>5</sup> According to Table III, spectral slopes between 3.6–3.9 were obtained between 5–25 MHz, whatever the shear rate. In the experimental study of Yuan and Shung,<sup>5</sup> the fibrinogen concentration was changed to promote the formation of RBC aggregates in tube flow. The current simulations are in agreement with the experimental results reported by others,<sup>5</sup> although the type of flow (tube versus Couette flow) and the geometry of the scattering ROI (3D versus 2D for the current simulations) differed between both studies. At frequencies between approximately 40–60 MHz, attenuation-compensated spectral slopes varying between 0.4–1.4 were measured experimentally at low shear rates for normal human blood.<sup>8,9</sup> To our knowledge, these results on whole-blood backscattering are the only ones available in the literature in this range of frequency. Although they may be erroneous because they were obtained with focused wideband transducers (by definition, a monochromatic plane wave should be used to measure the backscattering coefficient in steradian-cm<sup>-1</sup>), it may be worth mentioning that these slopes between 0.4–1.4 are within the range of values reported in Table III for shear rates of 0.1 and 0.05 s<sup>-1</sup>.

## D. Comparison to other modeling strategies

Models were proposed to predict the frequency dependence of ultrasound backscattering from the microstructure of soft biological tissues.<sup>1,4,22,23</sup> The different modeling strategies adopted in these studies are difficult to apply to a complex medium such as blood, because angulated fibers, aligned scatterers regularly spaced, independently distributed particles, isotropic media, or dilute systems of particles are poor descriptors of aggregated packed RBCs. The modeling of blood scattering is quite complex due to the high density of scatterers, the phenomenon of RBC aggregation, and the flow dependency of the scatterers' position. To our knowledge, very few studies addressed the issue of modeling blood scattering as a function of the frequency.

In 1999, the acoustic framework of the current model was proposed to study ultrasound backscattering from non-aggregated RBCs at hematocrits of 0%–100%, and frequencies of 2–500 MHz.<sup>10</sup> The effect of both the scatterers' shape and positioning on the backscattered power was studied in 3D. The mathematical relationship between the positioning of RBCs (function  $N$ ) and the structure factor was given in that study. Because the ROI was infinite, a narrow-band signal could be used ( $\psi_y = 0.21$  mm, bandwidth  $\approx 0.7$  MHz) and the filtering artifact produced by the frequency response of the transducer was limited. In Savéry and Cloutier,<sup>24</sup> the backscattering coefficient (monochromatic plane wave) was determined analytically for 3D diluted suspensions of RBC aggregates modeled as Gaussian-shaped inhomogeneities being either isotropic or anisotropic. The non-Rayleigh changes in the spectral slope were observed as the frequency or scatterers' size were increased. Recently, a totally different modeling strategy was adopted by the same authors to consider the positioning of RBCs forming aggregates.<sup>12</sup> Instead of using aligned Gaussian-shaped particles,<sup>24</sup> the Neyman–Scott point process was proposed to simulate RBC clustering in 3D. A monochromatic plane wave was considered in that study, but a limitation was the validity of the model at only a low hematocrit ( $<5\%$ ), as the exclusion volume effect was not taken into account. Very interestingly, the changes in the spectral slope found in the current study, as a function of the level of RBC aggregation, were also noticed in the previous 3D model at 5% hematocrit.<sup>12</sup> This suggests that the current 2D model may adequately describe the frequency dependence of ultrasound backscattering by blood. However, we are aware that the current model would have to be developed in 3D to satisfactorily describe the backscattering behavior as a function of the hematocrit.

## V. CONCLUSION

By using a microrheological iterative model previously developed,<sup>14</sup> various structures of RBC aggregates at a physiological hematocrit of 40% were obtained by varying the flow shear rate between Couette cylinders. Simulations were performed over a wide range of frequencies (5–120 MHz) for shear rates varying between 0.05 and 2 s<sup>-1</sup>. The main prediction of the model is that the growing of RBC aggregates at low shear rates causes an increase in the backscattered power at low frequencies ( $< 30$  MHz), and a diminution of the spectral slope (backscattered power versus frequency on a log–log scale) at frequencies between 30–90 MHz, approximately. Additional studies may be required to fully understand the backscattering behavior above 120 MHz. Another observation of the model is the important angular dependencies of the backscattered power at frequencies between 5–25 MHz. At higher frequencies, anisotropy of the backscattered power may still exist depending on the shear rate (level of RBC aggregation and spatial organization of RBCs). Consequently, it can be concluded that a scalar index, such as the mean size of the scatterers, may not fully characterize the phenomenon of RBC aggregation. The anisotropic behavior of the backscattered power and spectral slope may be other parameters to consider.

According to the results of the present study, the following question can be raised. For a giveninsonification angle, does the combination of measurements performed at low and high frequencies bring more information to the characterization of RBC aggregation? It appears, from the results, that the variations in backscattered power, spectral slope, and anisotropy convey complementary information. Dual frequency characterization was proposed before to characterize other types of biological tissue. The detection of malignant liver tumors, kidney microstructures, and vascular emboli are some examples.<sup>4,25,26</sup> The use of dual frequency may be a direction to proceed in the future.

## ACKNOWLEDGMENTS

This work was supported by operating grants from the Institutes of Health Research of Canada (No. MOP-36467) and the Heart and Stroke Foundation of Quebec, and by a research scholarship from the Fonds de la Recherche en Santé du Québec. The authors would like to acknowledge Mr. David Savéry for reviewing the manuscript.

- <sup>1</sup>K. K. Shung and G. A. Thieme, *Ultrasonic Scattering in Biological Tissues*, 1st ed. (CRC Press, Boca Raton, 1993).
- <sup>2</sup>F. S. Foster, C. J. Pavlin, K. A. Harasiewicz, D. A. Christopher, and D. H. Turnbull, "Advances in ultrasound biomicroscopy," *Ultrasound Med. Biol.* **26**(1), 1–27 (2000).
- <sup>3</sup>E. L. Madsen, F. Dong, G. R. Frank, B. S. Garra, K. A. Wear, T. Wilson, J. A. Zagzebski, H. L. Miller, K. K. Shung, S. H. Wang, E. J. Feleppa, T. Liu, W. D. O'Brien, Jr., K. A. Topp, N. T. Sanghvi, A. V. Zaitsev, T. J. Hall, J. B. Fowlkes, O. D. Kripfgans, and J. G. Miller, "Interlaboratory comparison of ultrasonic backscatter, attenuation, and speed measurements," *J. Ultrasound Med.* **18**(9), 615–631 (1999).
- <sup>4</sup>M. F. Insana, "Modeling acoustic backscatter from kidney microstructure using an anisotropic correlation function," *J. Acoust. Soc. Am.* **97**(1), 649–655 (1995).
- <sup>5</sup>Y. W. Yuan and K. K. Shung, "Ultrasonic backscatter from flowing whole blood. II. Dependence on frequency and fibrinogen concentration," *J. Acoust. Soc. Am.* **84**(4), 1195–1200 (1988).
- <sup>6</sup>H. Schmid-Schönbein, P. Gaetgens, and H. Hirsch, "On the shear rate dependence of red cell aggregation *in vitro*," *J. Clin. Invest.* **47**, 1447–1454 (1968).
- <sup>7</sup>M. S. Van Der Heiden, M. G. M. De Kroon, N. Bom, and C. Borst, "Ultrasound backscatter at 30 MHz from human blood: Influence of rouleau size affected by blood modification and shear rate," *Ultrasound Med. Biol.* **21**(6), 817–826 (1995).
- <sup>8</sup>G. R. Lockwood, L. K. Ryan, J. W. Hunt, and F. S. Foster, "Measurement of the ultrasonic properties of vascular tissues and blood from 35–65 MHz," *Ultrasound Med. Biol.* **17**(7), 653–666 (1991).
- <sup>9</sup>F. S. Foster, H. Obara, T. Bloomfield, L. K. Ryan, and G. R. Lockwood, "Ultrasound backscatter from blood in the 30 to 70 MHz frequency range," *IEEE Ultrasonics Symposium Proceedings*, 1599–1602 (1994).
- <sup>10</sup>I. Fontaine, M. Bertrand, and G. Cloutier, "A system-based approach to modeling the ultrasound signal backscattered by red blood cells," *Biophys. J.* **77**, 2387–2399 (1999).
- <sup>11</sup>I. Fontaine and G. Cloutier, "Frequency Dependence of Simulated Ultrasound Signals Backscattered by Aggregating Red Blood Cells," in *Acoustical Imaging*, edited by M. Halliwell and P. N. T. Wells (Kluwer Academic/Plenum, New York, 2000), pp. 297–302.
- <sup>12</sup>D. Savéry and G. Cloutier, "A point process approach to assess the frequency dependence of ultrasound backscattering by aggregating red blood cells," *J. Acoust. Soc. Am.* **110**(6), 3252–3262 (2001).
- <sup>13</sup>B. G. Teh and G. Cloutier, "The modeling and analysis of ultrasound backscattering by red blood cell aggregates with a system-based approach," *IEEE Trans. Ultrason. Ferroelectr. Freq. Control* **47**(4), 1025–1035 (2000).
- <sup>14</sup>I. Fontaine, D. Savéry, and G. Cloutier, "Simulation of ultrasound backscattering by red cell aggregates: Effect of shear rate and anisotropy," *Biophys. J.* **82**(4), 1696–1710 (2002).

- <sup>15</sup>L. Y. L. Mo and R. S. C. Cobbold, "Theoretical Models of Ultrasonic Scattering in Blood," in *Ultrasonic Scattering in Biological Tissues*, edited by K. K. Shung and G. A. Thieme (CRC Press, Boca Raton, 1993), Chap. 5, pp. 125–170.
- <sup>16</sup>G. Cloutier and Z. Qin, "Ultrasound backscattering from nonaggregating and aggregating erythrocytes—A review," *Biorheology* **34**(6), 443–470 (1997).
- <sup>17</sup>V. Twersky, "Transparency of pair-correlated, random distributions of small scatterers, with application to the cornea," *J. Opt. Soc. Am.* **65**(5), 524–530 (1975).
- <sup>18</sup>L. Allard, G. Cloutier, and L. G. Durand, "Effect of the insonification angle on the Doppler backscattered power under red blood cell aggregation conditions," *IEEE Trans. Ultrason. Ferroelectr. Freq. Control* **43**(2), 211–219 (1996).
- <sup>19</sup>I. Y. Kuo and K. K. Shung, "High frequency ultrasonic backscatter from erythrocyte suspension," *IEEE Trans. Biomed. Eng.* **41**(1), 29–34 (1994).
- <sup>20</sup>J. A. Campbell and R. C. Waag, "Ultrasonic scattering properties of three random media with implications for tissue characterization," *J. Acoust. Soc. Am.* **75**(6), 1879–1886 (1984).
- <sup>21</sup>J. F. Chen, J. A. Zagzebski, and E. L. Madsen, "Experimental demonstration of the frequency dependence of the effective scatterer number density," *J. Acoust. Soc. Am.* **99**(4), 1932–1936 (1996).
- <sup>22</sup>M. F. Santarelli and L. Landini, "A model of ultrasound backscatter for the assessment of myocardial tissue structure and architecture," *IEEE Trans. Biomed. Eng.* **43**(9), 901–911 (1996).
- <sup>23</sup>J. H. Rose, M. R. Kaufmann, S. A. Wickline, C. S. Hall, and J. G. Miller, "A proposed microscopic elastic wave theory for ultrasonic backscatter from myocardial tissue," *J. Acoust. Soc. Am.* **97**(1), 656–668 (1995).
- <sup>24</sup>D. Savéry and G. Cloutier, "Modeling of the Acoustic Signal Backscattered by a Biphasic Suspension: Application to the Characterization of Red Blood Cell Aggregation," in *Acoustical Imaging*, edited by M. Halliwell and P. N. T. Wells (Plenum, New York, 2000), pp. 289–295.
- <sup>25</sup>G. Sommer, E. W. Olcott, and L. Tai, "Liver tumors: Utility of characterization at dual-frequency US," *Radiology* **211**(3), 629–636 (1999).
- <sup>26</sup>M. A. Moehring and J. A. Ritcey, "Sizing emboli in blood using pulse Doppler ultrasound. I. Verification of the EBR model," *IEEE Trans. Biomed. Eng.* **43**(6), 572–580 (1996).